Phanerozoic evolution of atmospheric methane

Oliver Bartdorff,[1] Klaus Wallmann,[1,2] Mojib Latif,[2,3] and Vladimir Semenov[3]

Received 3 April 2007; revised 25 August 2007; accepted 3 October 2007; published 7 February 2008.

[1] A simple geochemical box model for the global cycle of methane (CH_4) has been developed and applied to reconstruct the evolution of atmospheric CH_4 over the entire Phanerozoic. According to the model, the partial pressure of atmospheric CH_4 (pCH_4) increased up to approximately 10 ppmv during the Carboniferous coal swamp era. This implies a maximum radiative forcing of about 3.5 W m^{-2} via CH_4. Through its radiative forcing, CH_4 heated the average global surface temperature by up to 1°C. The elevated pCH_4 values during the Permian-Carboniferous cold period may have moderated the temperature decline caused by the coeval drawdown of atmospheric CO_2. Additional runs with a global carbon model indicate that the heating induced by elevated pCH_4 favored the drawdown of atmospheric pCO_2 via enhanced rates of silicate weathering. Simulations with a state-of-the-art climate model reveal that the effects of atmospheric CH_4 on average global surface temperature also depend on the partial pressures of CO_2. The CH_4 climate effect is amplified by high background levels of atmospheric CO_2 such that a coeval increase in the partial pressure of both greenhouse gases has a much stronger climate effect than previously anticipated.

Citation: Bartdorff, O., K. Wallmann, M. Latif, and V. Semenov (2008), Phanerozoic evolution of atmospheric methane, *Global Biogeochem. Cycles*, *22*, GB1008, doi:10.1029/2007GB002985.

1. Introduction

[2] CH_4 is the most abundant hydrocarbon gas in the atmosphere and plays an important role in climate regulation [*Seinfeld and Pandis*, 1998]. It probably was one of the greenhouse gases, emitted by methanogenic bacteria, which warmed the early Earth surface to unexpected high temperatures [*Pavlov et al.*, 2000]. Being a greenhouse gas, CH_4 molecules let pass short-wave radiation, such as UV radiation but trap reflected outgoing long-wave radiation from the Earth's surface [*Fogg*, 2003]. Thus the troposphere gets warmer while the CH_4 content increases, the direct effect of CH_4 on the average global surface temperature [*Lelieveld et al.*, 1998]. Furthermore, an increase in tropospheric CH_4 affects the atmospheric partial pressures of carbon dioxide (pCO_2) and water vapor in the stratosphere and the tropospheric ozone concentration [*Blake and Rowland*, 1988]. These changes force additional global warming [*Harvey*, 1993], the indirect effect of CH_4 on the average global surface temperature [*Gassmann*, 1994].

[3] Except for the anthropogenic emission, CH_4 is emitted from waterlogged soils, by insects, out of the photic zone of the oceans and the deep seafloor, from shallow water regions of the oceans, out of lakes [*Berner and Berner*, 1996], from mud volcanoes [*Kopf*, 2003], and during magmatic degassing [*Ehhalt*, 1974]. In prehuman times, wetlands, particularly swamps and peat, were the prime emitters. In times of reduced terrestrial plant coverage, mud volcanoes might have been the most important CH_4 source [*Kopf*, 2003].

[4] CH_4 both affects climate and is affected by climate. Because of the impact of atmospheric CH_4 on climate [*Lelieveld et al.*, 1998] on both long and short timescales, several models for the global CH_4 cycle have been developed. These include models addressing tropospheric CH_4 oxidation [*Jacob*, 2003], modern atmospheric CH_4 change [*Dlugokencky et al.*, 1998], the future evolution of atmospheric CH_4 [*Dickinson and Cicerone*, 1986], and Precambrian pCH_4 levels [*Pavlov et al.*, 2003].

[5] In this article we attempt the first detailed reconstruction of the pCH_4 level over the entire Phanerozoic (570 Ma) with the main focus on biological sources. With our new model we also evaluate the possible effects of CH_4 on Phanerozoic climate evolution. We show that the Phanerozoic pCH_4 passes through significant changes, inducing noticeable shifts in climatic conditions.

2. Setup of the CH_4 Model

[6] The box model presented in this article is built on previous models of the global carbon cycle [*Wallmann*, 2001a, 2004]. New parameterizations are introduced to simulate the global CH_4 cycle. Hence fluxes of CH_4 into the atmosphere are related to external parameters such as changes in land area, land plant coverage, organic matter burial, and volcanic/tectonic activity. A simple model of

[1]Collaborative Research Center 574, University of Kiel, Kiel, Germany.
[2]Leibniz Institute of Marine Sciences, University of Kiel, Kiel, Germany.
[3]Collaborative Research Center 460, University of Kiel, Kiel, Germany.

0886-6236/08/2007GB002985

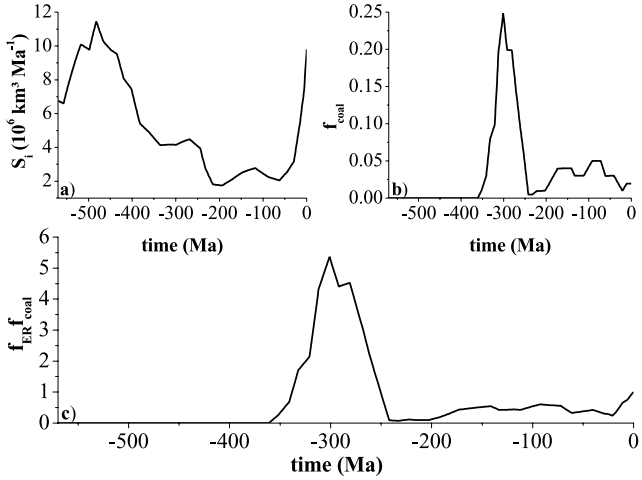

Figure 1. Changes in (a) sedimentation rate (S_i) [*Berner and Kothavala*, 2001], (b) coal fraction of terrigenous sediments (f_{coal}) [*Berner*, 2004], and (c) relative coal accumulation ($f_{ER}f_{coal}$) derived from Figures 1a and 1b and normalized on Pliocene value (see text).

atmospheric CH_4 oxidation is included to calculate, finally, the pCH_4 over the entire Phanerozoic and the radiative forcing (RF) induced by this greenhouse gas.

2.1. Sources of Atmospheric CH_4

[7] Atmospheric CH_4 is mainly released from biological sources hosted in terrestrial anoxic environments. Our understanding of atmospheric CH_4 cycling is, however, to a large extent limited by a poor quantification of these and other sources.

2.1.1. Wetlands

[8] Wetlands are the main recent natural sources of atmospheric CH_4. Direct records of the distribution of ancient wetlands are lacking. Coals are, however, formed from terrestrial plant material deposited in swamps and wetlands. Coals and coal basin sediments, which are preserved in the geological record, are thus a proxy for the abundance of methane-producing wetlands in the past.

[9] *Ronov* [1993] investigated the abundance of terrigenous sedimentary rocks, including coal basin sediments, deposited over the various periods of the Phanerozoic and preserved until today (S_p). These data were later updated and recompiled by W. W. Hay (personal communication, 2003) and applied by *Berner and Kothavala* [2001] and *Berner* [2004]. It should be considered that a large fraction of the initially deposited sediments was not preserved but was converted into metamorphic rocks and was lost by erosion and subduction. Previous studies on sedimentary rock cycling showed that this loss follows a simple first-order decay law [*Veizer and Jansen*, 1979]. Hence the initial terrigenous sedimentation rate S_i was calculated as [*Wallmann*, 2001a]

$$S_i = S_p e^{bt}, \tag{1}$$

using the S_P values listed by *Berner and Kothavala* [2001] while the decay constant b was set to the value 5×10^{-3} Ma^{-1} previously derived by *Gregor* [1985] and *Wallmann* [2001a]. A single b is appropriate to describe the loss of terrigenous sediments since the formation of coal swamps during the Carboniferous. The resulting S_i values plotted in Figure 1a were then multiplied with the fraction of terrigenous sediments deposited in coal basins (Figure 1b) taken from *Berner* [2004] to calculate the accumulation rate of coal basin sediments over the Phanerozoic. These values were finally normalized to the values derived for the most recent period considered in Ronov's compilations (the Pliocene) to calculate the relative change in coal basin sedimentation over the Phanerozoic ($f_{ER}f_{coal}$, Figure 1c). With this normalization we assume that the Quaternary sedimentation rate is close to the Pliocene value as suggested by recent studies [*Clift*, 2006].

[10] *Christensen et al.* [2003] investigated the CH_4 production in wetlands at different soil temperatures. Their data show an exponential growth in the production rate of CH_4 with increasing temperature (Figure 2a). We normalized this exponential dependency to the Quaternary average global surface temperature of about 13.5°C [*Wallmann*, 2001b] to describe the relative influence of ambient temperature on the CH_4 emission from waterlogged soils. We choose a simple exponential function to describe this dependency (Figure 2b). Thus the dimensionless temperature-dependent parameter ($f_{T\text{wetland}}$) for CH_4 production in waterlogged soils can be described as

$$f_{T\text{wetland}} = 0.111e^{0.1635\times\text{Temp}}, \tag{2}$$

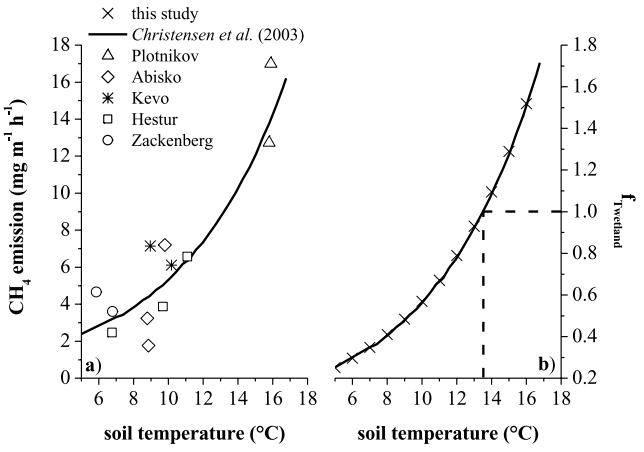

Figure 2. Dependency of CH_4 emission from waterlogged soils on ambient temperature (a) according to *Christensen et al.* [2003] and (b) normalized to the Quaternary average global surface temperature (13.5°C). An exponential function was fitted through the data to calculate the CH_4 emission from wetlands as a function of temperature ($f_{T\text{wetland}}$). Dashed lines indicate that the equation yields $f_{T\text{wetland}} = 1$ for the Quaternary global average surface temperature.

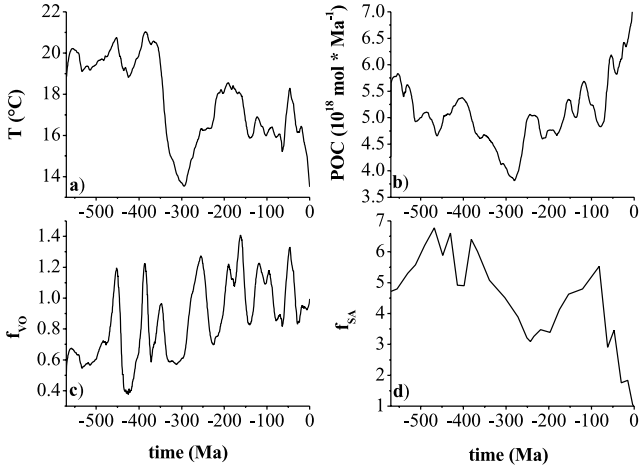

Figure 3. Changes in (a) average global surface temperature [*Wallmann*, 2004], (b) POC accumulation on the seafloor [*Wallmann*, 2004], (c) tectonic activity [*Wallmann*, 2004], and (d) normalized sea-covered area [*Ronov*, 1994] used as external forcings.

where the exponent "Temp" is the time-dependent average global surface temperature (Figure 3a) over the Phanerozoic calculated by *Wallmann* [2004]. For the Quaternary average global surface temperature this equation yields a value of unity so that $f_{T\text{wetland}}$ can be applied to calculate the effect of temperature change on CH_4 emissions from wetlands with respect to the recent temperature.

[11] The CH_4 production in ancient wetlands (F^{CH4}_{wetland}) is then calculated using the previously derived change in coal basin sedimentation ($f_{ER}f_{\text{coal}}$), the parameter $f_{T\text{wetland}}$ describing the effect of temperature on the CH_4 release from wetlands, and the recent CH_4 production rate of waterlogged soils and swamps [$F^{CH4}_{\text{wetland}}(q)$]

$$F^{CH_4}_{\text{wetland}} = F^{CH_4}_{\text{wetland}}(q) f_{ER} f_{\text{coal}} f_{T\text{wetland}}. \quad (3)$$

The modern value is estimated to fall into the range of 55–150 Tg CH_4 a^{-1} according to *Seinfeld and Pandis* [1998].

2.1.2. Insects

[12] Another important source of modern CH_4 is insects, mainly termites, producing 20 Tg CH_4 a^{-1} [*Intergovernmental Panel on Climate Change (IPCC)*, 2001]. Since the first appearance of insects these animals have influenced the pCH_4 in the atmosphere [*Grimaldi*, 2001]. There are, however, a lot of uncertainties about the evolution and abundance of ancient insects and their alkane production rate. In the model we assume that termites have been the main emitter of CH_4 of all insects, and we couple the evolution of termites and their recent CH_4 emission value [$F^{CH4}_{\text{termite}}(q)$] to calculate their Phanerozoic emission rate:

$$F^{CH_4}_{\text{termite}} = f_{IN} F^{CH_4}_{\text{termite}}(q). \quad (4)$$

The evolution of termites began in the Cretaceous [*Grimaldi*, 2001]. Hence the parameter f_{IN} is set to zero for the Paleozoic and early Mesozoic and is increased to 1 during the Cretaceous.

2.1.3. Magmatic Degassing

[13] The volcanic CH_4 emissions into the atmosphere by recent continental magmatic volcanism are rather small (0.8–6.2 Tg CH_4 a^{-1}) [*Judd et al.*, 2002]. To calculate the volcanic CH_4 release over the Phanerozoic, we assume the CH_4 emission via volcanism to be proportional to the activity of magmatic volcanoes. Thus the recent emissions of volcanoes [$F^{CH4}_{\text{volcano}}(q)$] and the calculated trend in activity of the continental volcanoes (f_{VO}) over time (Figure 3c) [*Wallmann*, 2004] give the following expression for the emission in the past:

$$F^{CH_4}_{\text{volcano}} = f_{VO} F^{CH_4}_{\text{volcano}}(q). \quad (5)$$

2.1.4. Plants

[14] Recent studies [*Keppler et al.*, 2006] have discovered that land plants emit substantial amounts of CH_4 into the atmosphere. *Keppler et al.* [2006] propose that the amount of plant-derived CH_4 accounts for 10–30% of the recent annual world CH_4 emission. The CH_4-producing processes in plants remain, however, enigmatic. The plant emissions are not considered in the model since a valid parameterization of this important methane source is currently not available.

2.1.5. Oceans

[15] Compared to the modern terrestrial emissions, the marine realm plays a minor role. The recent CH_4 release from the photic zone of the oceans (10–15 Tg CH_4 a^{-1}) [*IPCC*, 2001] is mainly driven by the biogenic production in anoxic microenvironments located in "marine snow" particles sinking through the upper water column. The accumulation rate of particulate organic carbon (POC) is used to define the CH_4 release from sinking particles in the upper water column because the methane-generating particle flux is reflected in marine POC accumulation:

$$F^{CH_4}_{\text{ocean}} = \frac{F^{\text{POC}}_B}{F^{\text{POC}}_B(q)} F^{CH_4}_{\text{ocean}}(q), \quad (6)$$

where F^{POC}_B is the burial rate used as a proxy for biological productivity of the oceans over time (Figure 3b), $F^{\text{POC}}_B(q)$ is the Quaternary burial rate of POC at the seafloor (7×10^{18} mol C Ma^{-1}) [*Wallmann*, 2003], and $F^{CH4}_{\text{ocean}}(q)$ is the recent CH_4 release from the photic zone of the oceans.

2.1.6. Continental Shelf

[16] Marine CH_4 generated in the pore space of sediments migrates toward the sediment surface, where it is oxidized by microbes or escapes through natural gas seeps as dissolved CH_4 or free gas. Some of this CH_4 is emitted into the atmosphere from shallow water environments such as marginal seas and mud flats. According to *Judd et al.* [2002], the amount of CH_4 released in shallow water environments is influenced by sea level change. During a falling sea level these potential CH_4 production areas

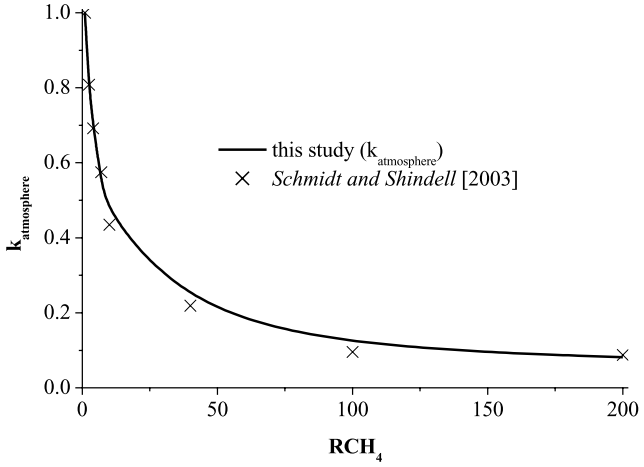

Figure 4. Decrease in loss rate of atmospheric CH_4 as a function of the atmospheric CH_4 concentration ($k_{atmosphere}$) [*Schmidt and Shindell*, 2003].

decrease whereas transgression increases the size of shallow water environments. Thus we constrain the changing size of the shelf-bounded sources over time by simply coupling the recent CH_4 emission rate of these environments with the change of shelf area covered by the oceans over time and the changing rate of POC burial:

$$F_{\text{shelf}}^{\text{CH}_4} = F_{\text{shelf}}^{\text{CH}_4}(q) f_{\text{SA}} \frac{F_B^{\text{POC}}}{F_B^{\text{POC}}(q)}, \tag{7}$$

where f_{SA} is the proxy data [*Ronov*, 1994] for the water-covered shelf area over time normalized to the recent value (Figure 3d) and $F_{\text{shelf}}^{\text{CH4}}(q)$ (0.4–12.2 Tg CH_4 a^{-1}) [*Judd et al.*, 2002] is the recent emission of CH_4 out of shallow water environments.

2.1.7. Mud Volcanoes

[17] Some CH_4 generated in the pore space of sediments is emitted during quiescent and eruptive periods from mud volcanoes, placed mainly along convergent plate margins where fluid-rich sediments accumulate [*Kopf*, 2002]. Mud volcanoes located on land and at shallow water depth emit substantial amounts of CH_4 into the atmosphere [*Etiope and Milkov*, 2004]. Deep-sea mud volcanoes with a global emission rate of about 0.1 Tg CH_4 a^{-1} [*Wallmann et al.*, 2006] are probably less important because CH_4 is almost completely oxidized near the seafloor and in the water column [*Mau et al.*, 2006]. The main controlling factor on mud volcanism is probably the rate and spatial extent of subduction and plate convergence providing the pressure gradients for fluid and mud ascent. Therefore we calculate the evolution of the CH_4 release from mud volcanoes for the past by using the recent CH_4 emission from mud volcanoes and the changing rates of subduction and organic matter accumulation:

$$F_{\text{mud}}^{\text{CH}_4} = F_{\text{mud}}^{\text{CH}_4}(q) \frac{F_B^{\text{POC}}}{F_B^{\text{POC}}(q)} f_{\text{VO}}, \tag{8}$$

where $F_{\text{mud}}^{\text{CH4}}(q)$ is the recent emission of CH_4 via mud volcanism, including both quiescent and eruptive degassing (6–9 Tg CH_4 a^{-1}) [*Etiope and Milkov*, 2004] and f_{VO} (Figure 3d) is the calculated tectonic/volcanic activity over the entire Phanerozoic [*Wallmann*, 2004].

2.1.8. CH_4 Release

[18] In our model the overall prehuman CH_4 emission into the atmosphere is thus given as (equations (2)–(8))

$$F_{\text{release}}^{\text{CH}_4} = F_{\text{mud}}^{\text{CH}_4} + F_{\text{volcano}}^{\text{CH}_4} + F_{\text{ocean}}^{\text{CH}_4} + F_{\text{shelf}}^{\text{CH}_4} + F_{\text{wetland}}^{\text{CH}_4} + F_{\text{termite}}^{\text{CH}_4}. \tag{9}$$

2.2. Sinks of Atmospheric CH_4

[19] The main destruction of CH_4 reaching the modern atmosphere takes place in the troposphere (360–530 Tg CH_4 a^{-1}) [*Seinfeld and Pandis*, 1998] because more than 80% [*Sudo et al.*, 2002] of the cleaning power of the atmosphere is housed in its lower 16 km [*Budyko et al.*, 1987]. A minor part of atmospheric CH_4 is consumed within soils.

2.2.1. CH_4 Oxidation in the Atmosphere

[20] Some of the reactants in the reaction chain of CH_4 destruction are formed in the troposphere, e.g., NO [*Jacob*, 2003]; some others, e.g., O_3, one of the main agents in tropospheric chemistry [*Wang et al.*, 1998], move from the stratosphere into the troposphere [*Schultz et al.*, 1999]. There are two types of triggers for the whole reaction chain of CH_4 destruction/oxidization: One is the solar flux, which triggers the photolytic reactions, and the other one is the radicals, which affect the chain reaction. The reaction chain for the production of the oxidizing agents is very complex and is discussed by *Seinfeld and Pandis* [1998]. The main oxidizing agents removing CH_4 from the atmosphere are hydroxyl radicals (OH) produced in these chain reactions [*Dunlop and Tully*, 1993]. Furthermore, *Johnson et al.* [2001] show that the CH_4 destruction by OH is linked to climate since both the OH production and the reaction of OH with CH_4 increase with temperature. The reaction efficiency of OH with CH_4 as a function of the average global surface temperature can be approximated by an Arrhenius expression [*Atkinson*, 2003]. The net effects of climate on the atmospheric production and consumption of OH radicals are, however, poorly understood and are therefore not considered in the model.

[21] In the context of our model it is important to note that the effectiveness of the CH_4 oxidation by OH increases as the amount of the hydrocarbon molecules decreases [*Jacob*, 2003; *Lawrence et al.*, 2001]. Because of the rapid recycling rate of OH at moderate CH_4 levels the oxidization processes mentioned above do not significantly deplete the OH [*Lelieveld et al.*, 2002]. However, at high CH_4 concentrations the cleaning power of the atmosphere decreases substantially. Consequently, the atmosphere adjusts to pollution when moderate CH_4 emissions prevail, while CH_4 accumulates in the atmosphere during times of enhanced emission.

[22] The loss of CH_4 from the atmosphere ($F_{\text{atmosphere}}^{\text{CH4}}$) normalized to the preindustrial loss [$F_{\text{loss}}^{\text{CH4}}(q)$] is proportional

Table 1. RCH_4 as Function of the Net Release of Methane Normalized to the Prehuman Value

Net Release	RCH_4
0	0
0.1	0.1
0.5	0.5
1	1
2	2.5
3	4.5
4	7.548
5	12.3
6	18.5
7	25.8
8	35.2
9	49.6
10	76.1
12	129.4
15	180.9
20	250.4

to the atmospheric content of methane (RCH_4) and a kinetic constant ($k_{\text{atmosphere}}$), which also depends on RCH_4:

$$\frac{F^{CH_4}_{\text{atmosphere}}}{F^{CH_4}_{\text{loss}}(q)} = k_{\text{atmosphere}} RCH_4. \tag{10}$$

[23] *Schmidt and Shindell* [2003] applied atmospheric chemistry modeling to quantify the exponential decrease in atmospheric OH abundance and CH_4 oxidation caused by increasing pCH_4 (Figure 4). Figure 4 shows the decreasing tropospheric oxidation with increasing atmospheric RCH_4. We fitted a third-order exponential term to the model results of *Schmidt and Shindell* [2003] to define a kinetic constant for atmospheric CH_4 oxidation depending on the prevailing atmospheric CH_4 level:

$$k_{\text{atmosphere}} = 0.07925 + 0.61712e^{\frac{-RCH_4}{5.43812}} + 0.62564e^{\frac{-RCH_4}{0.41025}} + 0.35927e^{\frac{-RCH_4}{39.436}}. \tag{11}$$

[24] The RCH_4 parameter appearing in this equation gives the pCH_4 in the atmosphere normalized to the preindustrial value (0.7 ppmv). We further assume that the preindustrial loss [$F^{CH4}_{\text{loss}}(q)$] and the preindustrial emission (225 Tg CH_4 a^{-1}) [*Schmidt and Shindell*, 2003] are balanced.

2.2.2. Oxidation Within Soils

[25] A small part (1–10%) [*Lelieveld et al.*, 1998] of the atmospheric CH_4, mainly the CH_4 in the soil air and/or in the air near the Earth's surface, is decomposed by soil organisms. These microorganisms live in the humus-rich and aerated part of soils. The humus layer is formed by land plants. Hence the methane oxidation rate in soils was much lower prior to the advent of land plants.

[26] *Berner and Kothavala* [2001] reconstructed the rise and evolution of vascular land plants over the Phanerozoic. These nondimensional data (f_{AN}) and the recent uptake of CH_4 by soil organisms ($F^{CH4}_{\text{soil}}(q)$ = 30–40 Tg CH_4 a^{-1}) [*King and Schnell*, 1994] are used to calculate the time-dependent CH_4 oxidation rate (F^{CH4}_{soil}) in the model:

$$F^{CH_4}_{\text{soil}} = F^{CH_4}_{\text{soil}}(q) f_{\text{AN}}. \tag{12}$$

2.2.3. Loss of Atmospheric CH_4

[27] CH_4 is decomposed because of oxidation processes in the atmosphere and within soils. Because of physical transport processes [*Ehhalt*, 1974], such as the Hadley circulation and eddy diffusion (together <60 Tg CH_4 a^{-1}), the reduction in the CH_4 inventory located in the lower atmosphere is not resolved in our model because of the lack of information on the atmospheric circulation processes in the Phanerozoic. We include this transported CH_4 mass (7–11% of total destroyed CH_4) [*Lelieveld et al.*, 1998] in the total recent chemical destruction processes of about 392–578 Tg CH_4 a^{-1} [*Seinfeld and Pandis*, 1998]. The destruction of CH_4 in the lower and upper atmosphere via the atmospheric cleaning power ($F^{CH4}_{\text{atmosphere}}$) and the uptake by soil organisms (F^{CH4}_{soil}) (equations (10) and (12)) can thus be described as

$$F^{CH_4}_{\text{loss}} = F^{CH_4}_{\text{soil}} + F^{CH_4}_{\text{atmosphere}}. \tag{13}$$

2.3. Budget of Atmospheric CH_4

[28] On the basis of the terms above (equations (9) and (13)) the changing inventory of CH_4 in the atmosphere over the Phanerozoic can be calculated as

$$\frac{d\text{MCH}_4}{dt} = F^{CH_4}_{\text{release}} - F^{CH_4}_{\text{loss}}, \tag{14}$$

where F^{CH4}_{release} is the total release of CH_4 into the atmosphere and F^{CH4}_{loss} is the consumption of atmospheric CH_4. Because of the fast consumption rate [*Jacob*, 2003] and the resulting short lifetime of CH_4 in the atmosphere [*Sudo et al.*, 2002], almost all of the released CH_4 gets decomposed. Thus the

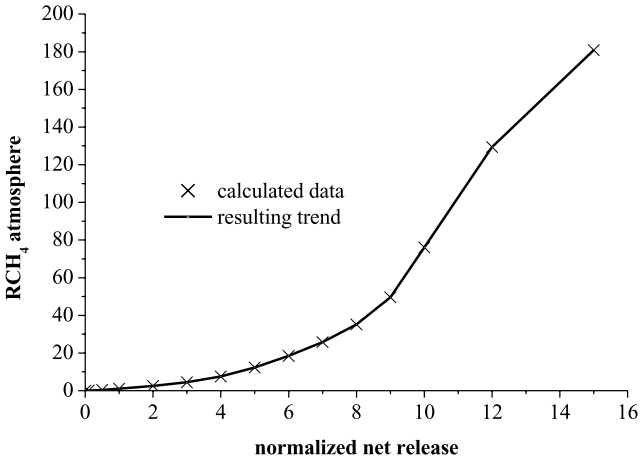

Figure 5. Atmospheric RCH_4 as a function of methane net release normalized to the preindustrial net release (compare Table 1).

Table 2. Parameter Values and Fluxes of Methane Considered in the Box Model[a]

Parameter	Description	Reference	Value
$pCH_4(p)$	preindustrial partial pressure of CH_4, ppmv	*Raynaud et al.* [1993]	(0.7)
$F_B{}^{POC}(q)$	Quarternary POC accumulation, 10^{18} mol Ma^{-1}	*Wallmann* [2004]	(7)
$F_{soil}{}^{CH4}(q)$	Quaternary CH_4 consumption of soils, 10^{18} mol Ma^{-1}	*IPCC* [2001]	(2.37)
$F_{termite}{}^{CH4}(q)$	Quaternary CH_4 release out of digestive tracks of insects, 10^{18} mol Ma^{-1}	*IPCC* [2001]	(1.25)
$F_{mud}{}^{CH4}(q)$	Quaternary CH_4 release out of mud volcanoes, 10^{18} mol Ma^{-1}	*Etiope and Milkov* [2004]	0.37–0.56 (0.56)
$F_{shelf}{}^{CH4}(q)$	Quaternary CH_4 release out of shallow water environments, 10^{18} mol Ma^{-1}	*Ehhalt and Heidt* [1973]	0.0436–0.873 (0.473)
$F_{volcano}{}^{CH4}(q)$	Quaternary CH_4 release out of terrestrial volcanoes, 10^{18} mol Ma^{-1}	*Judd et al.* [2002]	0.0499–0.387 (0.387)
$F_{ocean}{}^{CH4}(q)$	Quaternary CH_4 release out of the photic zone of the oceans, 10^{18} mol Ma^{-1}	*IPCC* [2001]	0.623–0.935 (0.935)
$F_{wetland}{}^{CH4}(q)$	Quaternary CH_4 release out of wetlands, particularly swamps, 10^{18} mol Ma^{-1}	*Seinfeld and Pandis* [1998]	3.43–9.35 (7.5)
$pCH_4(q)$	Quaternary partial pressure of CH_4, ppmv	*Raynaud et al.* [1993]	(0.355)
$pCO_2(q)$	Quaternary partial pressure of CO_2, ppmv	*Berner and Berner* [1996]	(230)

[a]Parameter values and fluxes applied in the standard case are given in parentheses.

atmospheric CH_4 amount ($F_{release}^{CH4} - F_{loss}^{CH4}$) is in a quasi steady state:

$$\frac{d\mathrm{MCH_4}}{dt} = 0, \tag{15}$$

$$F_{release}^{CH_4} - F_{soil}^{CH_4} - k_{atmosphere} F_{loss}^{CH_4}(q)\mathrm{RCH_4} = 0. \tag{16}$$

Solving for RCH_4 results in

$$\mathrm{RCH_4} = \frac{F_{release}^{CH_4} - F_{soil}^{CH_4}}{k_{atmosphere} F_{loss}^{CH_4}(q)}. \tag{17}$$

Considering a steady state also for the Quaternary methane cycle,

$$F_{loss}^{CH_4}(q) = F_{release}^{CH_4}(q) - F_{soil}^{CH_4}(q), \tag{18}$$

RCH_4 can be calculated as

$$\mathrm{RCH_4} = \frac{\text{net release}}{k_{atmosphere}}, \tag{19}$$

where "net release" is defined as the net release of methane into the atmosphere normalized to the Quaternary value:

$$\text{net release} = \frac{F_{release}^{CH_4} - F_{soil}^{CH_4}}{F_{release}^{CH_4}(q) - F_{soil}^{CH_4}(q)}. \tag{20}$$

Equation (19) is analytically unsolvable because of the exponents in the term $k_{atmosphere}$ (see equation (11)). Thus we solved this term numerically (Table 1 and Figure 5) with Mathematica 5.0. The normalized CH_4 concentration in the atmosphere is then calculated as a function of the net release (Figure 5): $(F_{release}^{CH4} - F_{soil}^{CH4})/[F_{release}^{CH4}(q) - F_{soil}^{CH4}(q)]$ = net release. RCH_4 increases exponentially with increasing net release.

2.4. Climate Effects of CH_4

[29] Atmospheric CH_4 is an important greenhouse gas and affects the average global surface temperatures by its radiative forcing (RF in W m^{-2}). The RF by CH_4 can be estimated as [*Thorpe et al.*, 1996]

$$\mathrm{RF} = 0.0411\left[\sqrt{p\mathrm{CH_4}} - \sqrt{p\mathrm{CH_4}(q)}\right], \tag{21}$$

where pCH_4 and $pCH_4(q)$ are the atmospheric partial pressures of CH_4 changing over time and the reference prehuman level (350 ppbv). In the absence of climate feedbacks the climate sensitivity parameter λ [0.30 K (W m^{-2})$^{-1}$] [*Seinfeld and Pandis*, 1998] can be used to calculate the impact of CH_4 on the average global surface temperature (ΔT^{CH4}):

$$\Delta T^{CH_4} = \lambda \mathrm{RF}. \tag{22}$$

3. Results and Discussion

[30] A standard run is produced, giving the evolution of methane-producing environments and of atmospheric CH_4

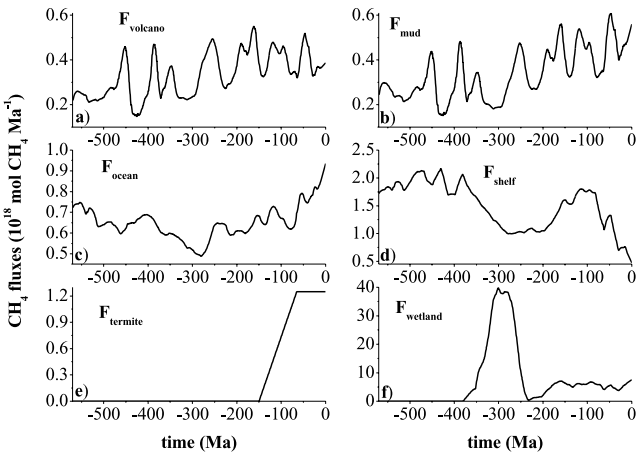

Figure 6. Changes in CH_4 fluxes into the atmosphere out of (a) magmatic volcanoes on land ($F_{volcano}$), (b) onshore and shallow water mud volcanoes (F_{mud}), (c) the photic zone of the oceans (F_{ocean}), (d) shelf zones, (e) digestive tracts of insects ($F_{termite}$), and (f) wetlands ($F_{wetland}$) used for the calculation of atmospheric pCH_4.

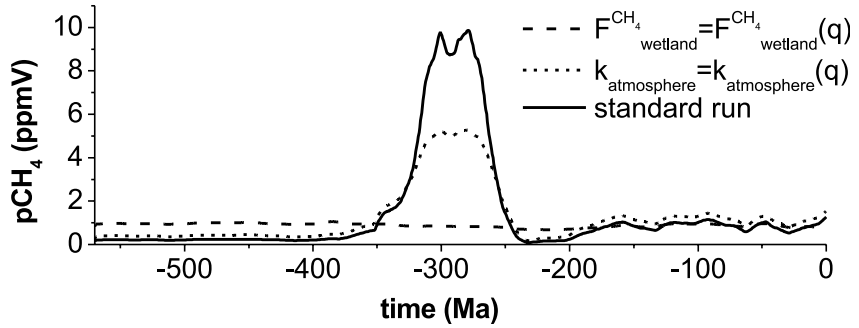

Figure 7. Changes in atmospheric partial pressure of methane (pCH_4) in the standard run and in sensitivity runs with a constant kinetic loss of CH_4 from the atmosphere [$k_{atmosphere} = k_{atmosphere}(q)$] and with constant wetland emissions [$F_{wetland}^{CH4} = F_{wetland}^{CH4}(q)$].

over the various periods of the Phanerozoic. Then the controls on pCH_4 are evaluated by using the results of the standard run and additional model runs (sensitivity tests) with systematically varied parameter values. Table 2 shows the prehuman emission rates applied in the standard run.

3.1. Phanerozoic Evolution of pCH_4

[31] This study is the first attempt to describe the atmospheric CH_4 evolution over the entire Phanerozoic. The corresponding CH_4 emission trends of the individual emitters are illustrated in Figures 6a–6f. Since the advent of land plants during the Paleozoic, swamps and wetland have been the main methane emitters. However, during the early Paleozoic the marine methane-producing environments were more significant (Figures 6b–6d) because of the lower terrestrial emission rates.

[32] In the standard run the CH_4 release reached the maximum value during the Carboniferous coal swamp era (Figure 6f). Consequently, the atmospheric pCH_4 increased to 10 ppmv (Figure 7) during the middle Phanerozoic. The next two peaks were reached in the Cretaceous and Jurassic, with maximum contents of 1.5 ppmv approaching the pCH_4 level prevailing in the modern atmosphere.

[33] The main trend in pCH_4 was influenced by the appearance of vascular land plants and the subsequent spread of swamps on the continents. The first land plants flourished on the continents during the Silurian. During the following Carboniferous and Permian, large continental areas were covered by wetlands, and vast amounts of CH_4 were formed in these swamps and wetlands by the microbial degradation of plant remains under anoxic conditions (Figure 6f). According to the standard run, the pCH_4 was up to 28 times higher than in prehuman times and six times higher than today during the Middle Phanerozoic (Figure 7).

[34] The importance of the wetland source is demonstrated by an additional model run where this main emitter was maintained at the low Quaternary level over the entire model period [$F_{wetland}^{CH4} = F_{wetland}^{CH4}(q)$]. The resulting Phanerozoic pCH_4 and RF trends showed only small variations, confirming that the model output is mainly controlled by methane emissions from wetlands (Figures 7 and 8).

3.2. Effects of Atmospheric CH_4 on Average Global Surface Temperature and pCO_2

[35] During the Carboniferous coal swamp era the rising pCH_4 level caused a strong positive RF (Figure 8), inducing a temperature increase of up to 1°C (Figure 9a). During periods of low CH_4 emission the temperature effect of methane was small whereas in times with high CH_4 emission rates and low atmospheric loss the effects became significant, especially during the Permian-Carboniferous coal swamp era.

[36] Additional model runs were performed with the carbon box model of *Wallmann* [2004] to explore the effects of CH_4-induced warming on global carbon cycling. The methane model presented in this paper was included in the CO_2 model of *Wallmann* [2004], which also considered the CO_2 produced by the oxidation of methane emitted from geological sources (volcanoes). The CO_2 produced through the oxidation of biogenic CH_4 wetlands is not considered since the biogenic CH_4 is part of the rapid biological carbon cycle (primary production, export production, and respiration) that is not resolved by the model. The secular temperature trend was calculated by adding the methane temperature term (equation (22)) to the temperature equation of *Berner and Kothavala* [2001]:

$$T = \Gamma \ln \mathrm{RCO_2} - W_s \frac{t}{-570} + T(q) + \mathrm{GEOG} + \Delta T^{\mathrm{CH_4}}, \quad (23)$$

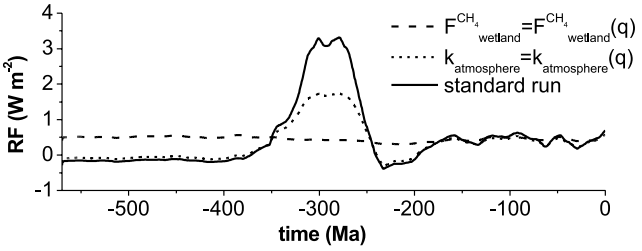

Figure 8. Changes in radiative forcing (RF) in the standard run and in sensitivity runs with a constant kinetic loss of CH_4 from the atmosphere [$k_{atmosphere} = k_{atmosphere}(q)$] and with constant wetland emissions [$F_{wetland}^{CH4} = F_{wetland}^{CH4}(q)$].

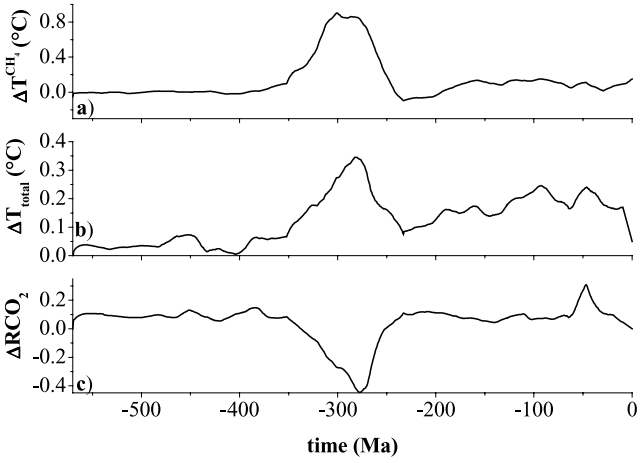

Figure 9. Changes in global average surface temperature over the Phanerozoic: (a) direct temperature change due to atmospheric CH_4 greenhouse gas effect, (b) temperature changes calculated in the model of *Wallmann* [2004] considering the impacts of CH_4 and CO_2, and (c) changes in RCO_2 induced by enhanced silicate weathering considering the effect of CH_4 on temperature.

where Γ gives the relation between surface temperature and RCO_2, RCO_2 is the atmospheric partial pressure of CO_2 normalized to the Quaternary value (230 μatm), W_s defines the impact of increasing solar luminosity on surface temperature, GEOG describes the effect of paleogeography on albedo and global surface temperature, and $T(q)$ is the Quaternary average global surface temperature (13.5°C).

[37] According to this new model, the warming induced by CH_4 enhances the consumption of CO_2 via silicate weathering. RCO_2 decreases during periods of enhanced CH_4 release (Figure 9c) because the magnitude of the CO_2 sink, induced by accelerated silicate weathering, surpasses the CO_2 production caused by methane oxidation. Nevertheless, average global surface temperatures were enhanced by 0.4°C because of the high methane emissions from wetlands during the Permian and Carboniferous. The long-lasting methane emissions during this coal swamp era may have prevented a global glaciation during the middle Phanerozoic. Short pulses of methane from dissociating gas hydrates might, in contrast, reduce the pCO_2 level beyond a critical value and could trigger ''snowball Earth'' events because methane has a much smaller atmospheric residence time than CO_2 [*Schrag et al.*, 2002].

3.3. CH_4 Oxidation in the Phanerozoic Atmosphere

[38] The increase in atmospheric CH_4 caused by high CH_4 emissions is further amplified by the coeval decrease in the cleaning power of the atmosphere. An additional model run with a time-independent kinetic constant for atmospheric CH_4 loss [$k_{atmosphere} = k_{atmosphere}(q)$] was performed to explore the effects of atmospheric oxidation. The high Quaternary value applied in this model run induced much lower pCH_4 and RF values over the Permian-Carboniferous and other periods of the Phanerozoic (Figures 7 and 8). Only during periods of very low methane emission, e.g., during the early Paleozoic, the calculated pCH_4 and RF are higher than in the standard run. The strong sensitivity of the model output with respect to the kinetic constant of atmospheric oxidation confirms that the Phanerozoic evolution of atmospheric pCH_4 is strongly affected by the nonlinear relation between CH_4 emissions and atmospheric cleaning power.

3.4. Effects of Atmospheric Methane in a State-of-the-Art Climate Model

[39] Mean global temperature and methane changes in global coupled climate simulations are in general comparable to the Phanerozoic era conditions and despite other differences in boundary conditions and external forcing may serve as a demonstration of comprehensive dynamical feedbacks in a fully coupled three-dimensional climate system model. Several climate change simulations with different greenhouse gas (GHG) concentrations have been performed with the global coupled atmosphere–ocean–sea ice general circulation model ECHAM5/MPI-OM [*Marsland et al.*, 2003; *Roeckner et al.*, 2003; *Semenov and Latif*, 2006]. The climate change experiments were performed relative to preindustrial climate conditions with atmospheric CO_2 and CH_4 concentrations of 280 and 0.76 ppmv, respectively. Five 200 year long simulations with (instantaneously) 10 and 20 times increased pCH_4, doubling of pCO_2, and their combined effects ($10 \times CH_4 + 2 \times CO_2$ and $20 \times CH_4 + 2 \times CO_2$) were performed. The simulations started from year 500 of a long control integration (performed at the Max Planck Institute for Meteorology) [*Gregory et al.*, 2005]. The global mean surface temperature in the control simulation amounts to about 14°C.

[40] The evolution of the simulated global annual mean surface air temperature (SAT) for the different simulations is shown in Figure 10. The SAT increases (last 30 years of the perturbed experiment) range from 0.75°C to 4.6°C. The time for the climate system to adjust to the perturbation in the GHG concentrations varies from 20 to 50 years (*e*-folding time for the weakest, $10 \times CH_4$, and the strongest, $20 \times CH_4 + 2 \times CO_2$, forcing, respectively). An estimate of

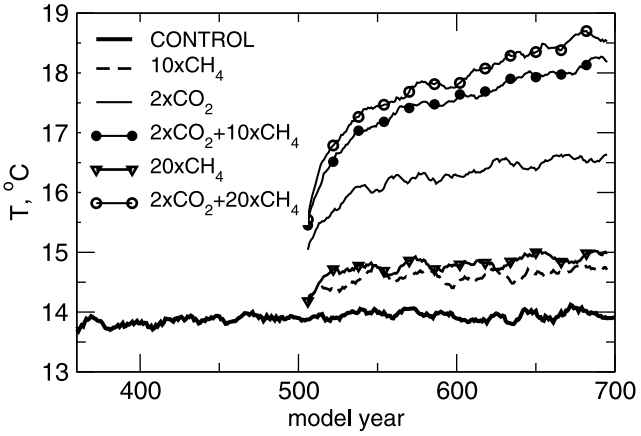

Figure 10. Global mean annual surface air temperatures (SAT), °C, as simulated by the ECHAM5/MPI-OM model in different climate change simulations (see legend). Eleven-year running means are shown.

the RF (top of atmosphere, first year) in the 10 × CH_4 experiment is 2.1 W m^{-2}, resulting in global SAT increase of 0.75°C. Interestingly, the further doubling of pCH_4 in the model practically does not change the global mean RF, resulting in an additional minor global SAT increase of 0.2°C. However, the regional differences (not shown) reach 3.5°C and are largest in the northern extratropics. In particular for the modern era climate conditions the simulations show a warming amplified by a factor of 4 in northern Eurasia where the largest wetlands are located. After adjustment of the SAT the SW RF significantly increases basically because of the total cloud cover decrease (about 0.9%/°C) and sea ice retreat (12%/°C). It is apparent from Figure 10 that the SAT changes in the simulations with increased pCH_4 and pCO_2 together are much stronger than adding the changes from the two individual simulations. The methane effect doubles roughly under 2 × pCO_2 conditions. This nonlinearity presumably arises from the water vapor feedback [*Held and Soden*, 2000]. However, the analysis of the spatial distribution of the SAT changes reveals that dynamical factors may also have a significant contribution. The largest temperature differences are found in the northern high latitudes in winter and are related to the sea ice changes. The latter are partly linked to changes in the large-scale ocean circulation reflected by strong surface water temperature anomalies in the Atlantic Ocean.

4. Conclusion

[41] The present model describes the secular atmospheric pCH_4 trend over the entire Phanerozoic and demonstrates the importance of the CH_4 emission from wetlands in the past. Atmospheric oxidation is able to compensate for moderate CH_4 emission rates, but with increasing pollution, methane accumulates in the atmosphere. In times of atmospheric CH_4 accumulation, methane has a significant effect on average global surface temperature and RCO_2. During times of high organic matter accumulation in terrestrial environments (Permian-Carboniferous coal swamp era) the atmospheric pCH_4 increases up to 10 ppmv. The high pCH_4 during this period implies a maximum RF of about 3.5 W m^{-2} via CH_4, which is twice as high as the RF currently caused by anthropogenic CO_2.

[42] The model results show, conspicuously, that RCO_2 did not increase in response to increasing CH_4 emissions. By its radiative forcing and because of its decomposition into CO_2, CH_4 heated the average global surface temperature by up to 1°C. The RCO_2 values were, however, substantially reduced by weathering processes which were accelerated by the CH_4-induced warming. Overall, CO_2 consumption via enhanced weathering surpassed CO_2 production via methane oxidation so that the atmospheric CO_2 level dropped in response to enhanced CH_4 emissions. As a net effect, the average global surface temperature increased by only 0.4°C during the Carboniferous coal swamp era.

[43] The elevated pCH_4 values during the Permian-Carboniferous cold period may have moderated the cooling trend caused by the coeval drawdown of atmospheric CO_2. Both the decrease in pCO_2 and the increase in pCH_4 are intimately linked to the spread of land plants during the Carboniferous and Permian. The high CH_4 emissions from swamps during these periods may have prevented the development of a snowball Earth state repeatedly encountered during the Precambrian prior to the advent of land plants.

[44] Simulations with a state-of-the-art climate model show that the effects of atmospheric CH_4 on average global surface temperature are amplified by high background levels of atmospheric CO_2. A coeval increase in the partial pressure of both greenhouse gases thus has a much stronger climate effect than previously anticipated.

[45] **Acknowledgments.** We are grateful to the SFB 574 "Volatiles and Fluids in Subduction Zones" at Kiel University for support of this work. We would also like to thank Bob Berner for his review and for sending us an unpublished manuscript on Phanerozoic methane cycling that he wrote 13 years ago.

References

Atkinson, R. (2003), Kinetics of the gas-phase reactions of OH radicals with alkanes and cycloalkanes, *Atmos. Chem. Phys.*, *3*, 2233–2307.
Berner, E. K., and R. A. Berner (1996), *Global Environment, Water, Air, and Geochemical Cycles*, Prentice-Hall, Upper Saddle River, N. J.
Berner, R. A. (2004), *The Phanerozoic Carbon Cycle: CO_2 and O_2*, 158 pp., Oxford Univ. Press, New York.
Berner, R. A., and Z. Kothavala (2001), GEOCARB III: A revised model of atmospheric CO_2 over Phanerozoic time, *Am. J. Sci.*, *301*, 182–204.
Blake, D. R., and F. S. Rowland (1988), Continuing worldwide increase in tropospheric methane, 1978 to 1987, *Science*, *239*, 1129–1131.
Budyko, M. I., A. B. Ronov, and A. L. Yanshin (1987), *History of the Earth's Atmosphere*, 139 pp., Springer, New York.
Christensen, T. R., A. Ekberg, L. Ström, M. Mastepanov, N. Panikov, M. Öquist, B. H. Svensson, H. Nykänen, P. J. Martikainen, and H. Oskarsson (2003), Factors controlling large scale variations in methane emissions from wetlands, *Geophys. Res. Lett.*, *30*(7), 1414, doi:10.1029/2002GL016848.
Clift, P. D. (2006), Controls on the erosion of Cenozoic Asia and the flux of clastic sediment to the ocean, *Earth Planet. Sci. Lett.*, *241*, 571–580.
Dickinson, R. E., and R. J. Cicerone (1986), Future global warming from atmospheric trace gases, *Nature*, *319*, 109–115.
Dlugokencky, E. J., K. A. Masarie, P. M. Lang, and P. P. Tans (1998), Continuing decline in the growth rate of atmospheric methane, *Nature*, *393*, 447–450.
Dunlop, J. R., and F. P. Tully (1993), A kinetic study of OH radical reactions with methane and perdeuterated methane, *J. Phys. Chem.*, *97*, 11,148–11,150.
Ehhalt, D. H. (1974), The atmospheric cycle of methane, *Tellus*, *26*, 58–70.
Ehhalt, D. H., and L. E. Heidt (1973), Vertical profiles of CH_4 in the troposphere and stratosphere, *J. Geophys. Res.*, *78*, 5265–5271.
Etiope, G., and A. V. Milkov (2004), A new estimate of global methane flux from onshore and shallow submarine mud volcanoes to the atmosphere, *Environ. Geol.*, *46*, 997–1002.
Fogg, P. G. T. (2003), General behaviour and origins of greenhouse and significant trace gases, in *Chemicals in the Atmosphere: Solubility, Sources and Reactivity*, edited by P. G. T. Fogg and J. M. Sangster, pp. 1–18, John Wiley, Hoboken, N. J.
Gassmann, F. (1994), *Was ist los mit dem Treibhaus Erde?*, Hochschulverlag, Zurich, Switzerland.
Gregor, C. B. (1985), The mass-age distribution of Phanerozoic sediments, in *The Chronology of the Geologic Record*, edited by N. J. Snelling, *Geol. Soc. London Mem.*, *10*, 284–289.
Gregory, J. M., et al. (2005), A model intercomparison of changes in the Atlantic thermohaline circulation in response to increasing atmospheric CO_2 concentration, *Geophys. Res. Lett.*, *32*, L12703, doi:10.1029/2005GL023209.
Grimaldi, D. (2001), Insect evolutionary history from Handlirsch to Hennig and beyond, *J. Paleontol.*, *75*, 1152–1160.
Harvey, L. D. D. (1993), A guide to global warming potentials (GWPs), *Energy Policy*, *21*, 24–34.
Held, I. M., and B. J. Soden (2000), Water vapor feedback and global warming, *Annu. Rev. Energy Environ.*, *25*, 441–475.

Intergovernmental Panel on Climate Change (IPCC) (2001), *Climate Change 2001: The Scientific Basis*, edited by J. T. Houghton et al., 881 pp., Cambridge Univ. Press, Cambridge, U. K.

Jacob, D. J. (2003), The oxidizing power of the atmosphere, in *Handbook of Weather, Climate and Water: Atmospheric Chemistry, Hydrology, and Societal Impacts*, edited by T. D. Potter and B. R. Colman, pp. 253–271, Wiley-Interscience, Hoboken, N. J.

Johnson, C. E., D. S. Stevenson, W. J. Collins, and R. G. Derwent (2001), Role of climate feedback on methane and ozone studied with a coupled ocean-atmosphere-chemistry model, *Geophys. Res. Lett.*, *28*, 1723–1726.

Judd, A. G., M. Hovland, L. I. Dimitrov, S. Garcia Gill, and V. Jukes (2002), The geological methane budget at continental margins and its influence on climate change, *Geofluids*, *2*, 109–126.

Keppler, F., J. T. G. Hamilton, M. Brass, and T. Roeckmann (2006), Methane emission from terrestrial plants under aerobic conditions, *Nature*, *439*, 187–191.

King, G. M., and S. Schnell (1994), Effect of increasing atmospheric methane concentration on ammonium inhibition of soil methane consumption, *Nature*, *370*, 282–284.

Kopf, A. J. (2002), Significance of mud volcanism, *Rev. Geophys.*, *40*(2), 1005, doi:10.1029/2000RG000093.

Kopf, A. J. (2003), Global methane emission through mud volcanoes and its past and present impact on the Earth's climate, *Int. J. Earth Sci.*, *92*, 806–816.

Lawrence, M. G., P. Jöckel, and R. Kuhlmann (2001), What does the global mean OH concentration tell us?, *Atmos. Chem. Phys.*, *1*, 37–49.

Lelieveld, J., P. J. Crutzen, and F. J. Dentener (1998), Changing concentration, lifetime and climate forcing of atmospheric methane, *Tellus, Ser. B*, *50*, 128–150.

Lelieveld, J., W. Peters, F. J. Dentener, and M. C. Krol (2002), Stability of tropospheric hydroxyl chemistry, *J. Geophys. Res.*, *107*(D23), 4715, doi:10.1029/2002JD002272.

Marsland, S. J., H. Haak, J. H. Jungclaus, M. Latif, and F. Röske (2003), The Max-Planck-Institute global ocean/sea ice model with orthogonal curvilinear coordinates, *Ocean Modell.*, *5*, 91–127.

Mau, S., H. Sahling, G. Rehder, E. Suess, and E. Soeding (2006), Estimates of methane output from mud extrusions at the erosive convergent margin off Costa Rica, *Mar. Geol.*, *225*, 129–144.

Pavlov, A. A., J. F. Kasting, L. L. Brown, K. A. Rages, and R. Freedmann (2000), Greenhouse warming by CH_4 in the atmosphere of early Earth, *J. Geophys. Res.*, *105*, 11,981–11,990.

Pavlov, A. A., M. T. Hurtgen, J. F. Kasting, and M. A. Arthur (2003), Methane-rich Proterozoic atmosphere?, *Geology*, *31*, 87–90.

Raynaud, D., J. Jouzel, J. M. Barnola, J. Chappellaz, R. J. Delmas, and C. Lorius (1993), The ice record of greenhouse gases, *Science*, *259*, 926–934.

Roeckner, E., et al. (2003), The atmospheric general circulation model ECHAM 5. part I: Model description, *MPI Tech. Rep. 349*, Max Planck Inst. for Meteorol., Hamburg, Germany.

Ronov, A. B. (1993), *Stratisfera: Ili Osadochnaya Obolochka Zemli (Kolichestvennoe Issledovanie)*, 144 pp., Nauka, Moscow.

Ronov, A. B. (1994), Phanerozoic transgressions and regressions on the continents: A quantitative approach based on areas flooded by the sea and areas of marine and continental deposition, *Am. J. Sci.*, *294*, 777–801.

Schmidt, G. A., and D. T. Shindell (2003), Atmospheric composition, radiative forcing, and climate change as a consequence of a massive methane release from gas hydrates, *Paleoceanography*, *18*(1), 1004, doi:10.1029/2002PA000757.

Schrag, D. P., R. A. Berner, P. F. Hoffmann, and G. P. Halverson (2002), On the initiation of a snowball Earth, *Geochem. Geophys. Geosyst.*, *3*(6), 1036, doi:10.1029/2001GC000219.

Schultz, M. G., et al. (1999), On the origin of tropospheric ozone and NO_x over the tropical South Pacific, *J. Geophys. Res.*, *104*, 5829–5844.

Seinfeld, J. H., and S. N. Pandis (1998), *Atmospheric Chemistry and Physics: From Air Pollution to Climate Change*, 1326 pp., John Wiley, Hoboken, N. J.

Semenov, V. A., and M. Latif (2006), Impact of tropical Pacific variability on the mean North Atlantic thermohaline circulation, *Geophys. Res. Lett.*, *33*, L16708, doi:10.1029/2006GL026237.

Sudo, K., M. Takahashi, and H. Akimoto (2002), CHASER: A global chemical model of the troposphere: 2. Model results and evaluation, *J. Geophys. Res.*, *107*(D21), 4586, doi:10.1029/2001JD001114.

Thorpe, R. B., K. S. Law, S. Bekki, and J. A. Pyle (1996), Is methane-driven deglaciation consistent with the ice core record?, *J. Geophys. Res.*, *101*, 28,627–28,635.

Veizer, J., and S. L. Jansen (1979), Basement and sedimentary recycling and continental evolution, *J. Geol.*, *87*, 341–370.

Wallmann, K. (2001a), Controls on the Cretaceous and Cenozoic evolution of seawater composition, atmospheric CO_2 and climate, *Geochim. Cosmochim. Acta*, *65*, 3005–3025.

Wallmann, K. (2001b), The geological water cycle and the evolution of marine $\delta^{18}O$ values, *Geochim. Cosmochim. Acta*, *65*, 2469–2485.

Wallmann, K. (2003), Feedbacks between oceanic redox states and marine productivity: A model perspective focused on benthic phosphorus cycling, *Global Biogeochem. Cycles*, *17*(3), 1084, doi:10.1029/2002GB001968.

Wallmann, K. (2004), Impact of atmospheric CO_2 and galactic cosmic radiation on Phanerozoic climate change and the marine $\delta^{18}O$ record, *Geochem. Geophys. Geosyst.*, *5*, Q06004, doi:10.1029/2003GC000683.

Wallmann, K., M. Drews, G. Aloisi, and G. Bohrmann (2006), Methane discharge into the Black Sea and the global ocean via fluid flow through submarine mud volcanoes, *Earth Planet. Sci. Lett.*, *248*, 544–599.

Wang, C., R. G. Prinn, and A. P. Sokolov (1998), A global interactive chemistry and climate model: Formulation and testing, *J. Geophys. Res.*, *103*, 3399–3418.

O. Bartdorff, Collaborative Research Center 574, University of Kiel, Wischhofstraße 1–3, D-24148 Kiel, Germany. (oliver.bartdorff@jrspet.com)

M. Latif and K. Wallmann, Leibniz Institute of Marine Sciences, University of Kiel, Düsternbrooker Weg 20, D-24105 Kiel, Germany. (mlatif@ifm-geomar.de; kwallmann@ifm-geomar.de)

V. Semenov, Collaborative Research Center 460, University of Kiel, Düsternbrooker Weg 20, D-24105 Kiel, Germany. (vsemenov@ifm-geomar.de)